THE ROYAL SOCIETY

Imaging of inversion twin boundaries in potassium titanyl phosphate (KTP) by liquid-crystal surface decoration and X-ray diffraction topography

By Chr. Scherf[1], Th. Hahn[1], G. Heger[1], N. R. Ivanov[2] and H. Klapper[3]

[1]*Institut für Kristallographie, RWTH Aachen, 52056 Aachen, Germany*
[2]*Shubnikov Institute of Crystallography, Russian Academy of Sciences, 59 Leninskii Prospect, Moscow 117333, Russia*
[3]*Mineralogisch-Petrologisches Institut, Universität Bonn, Poppelsdorfer Schloss, 53115 Bonn, Germany*

An extended inversion boundary separating two large 180° domains of a flux-grown KTP crystal is studied by nematic liquid-crystal (NLC) surface decoration and by X-ray projection and section topography using Mo-$K\alpha$ radiation. Although a non-polar (100) cleavage plate was used for NLC decoration, the domains appeared by bright optical contrast. The boundary exhibits a mainly irregular zigzag course with an—on average—charged orientation and is clearly visualized by both methods. It appears by strong contrast in X-ray reflection 004 (normal to the polar axis) and is completely invisible in reflection 040. A large uncharged planar boundary segment parallel to the polar axis and inclined by *ca.* 40° to the normal of the specimen surface shows in reflection 004 dynamical fringe contrast of the stacking fault type. A section topograph of this segment exhibits an ideal 'hourglass' contrast pattern, proving the absence of long-range strain and of any tilt of the reflecting (001) planes across the inversion boundary.

Keywords: potassium titanyl phosphate ($KTiOPO_4$); 180° domains; inversion boundary; liquid-crystal surface decoration; X-ray projection topography; section topography

1. Introduction

By definition, inversion domains occur only in non-centrosymmetrical crystals. Two categories of acentric crystal classes are distinguished: the ten pyroelectric classes and the eleven non-pyroelectric classes. Pyroelectric crystals possess a permanent (spontaneous) polarization which has opposite directions in inversion domains (180° domains). The highly important group of ferroelectric crystals belongs to this category. A well-known example of a non-pyroelectric crystal exhibiting inversion domains is quartz with its grown-in Brazil-twin domains.

Inversion domains can be detected directly, or indirectly by etching, by piezoelectric and electro-optic methods, and, in enantiomorphic crystals, by the reversal of

the optical-activity sense. Moreover, in pyroelectric crystals the decoration of oppositely polarized domains by suitable electrically charged powder or by nematic liquid crystals (NLC) is very useful. Besides these methods based on physical properties, diffraction imaging techniques such as X-ray diffraction topography or—for very thin crystals—transmission electron microscopy are applied to visualize inversion domain boundaries.

Potassium titanyl phosphate, $KTiOPO_4$ (KTP), is ferroelectric with point group $mm2$ and Curie temperature at 934 °C (transition to the centrosymmetrical point group mmm). Its 180° domains have been studied by etching (Satyanarayan & Bhat 1997), by pyroelectric decoration with electrostatic toners (Laurell *et al*. 1992; Wang *et al*. 1993), by anomalous-scattering topography (Huang *et al*. 1996; Hu *et al*. 1997) and by synchrotron radiation and conventional X-ray topography of twin inversion boundaries (180° walls) (Wang *et al*. 1993; Satyanarayan *et al*. 1995). An interesting study of periodic domain inversion in poled KTP by high-resolution X-ray topography has been published by Hu *et al*. (1996). In the present work we report a comparative study of an inversion boundary in KTP by liquid-crystal surface decoration and by conventional transmission X-ray diffraction topography.

2. Nematic liquid-crystal (NLC) surface decoration

The pyroelectric surface decoration of antipolar domains by charged particles goes back to Kundt (1883): the crystal is heated or cooled and sprayed with sulphur and minium (Pb_3O_4) powder. The yellow sulphur particles deposit on the positively charged surface regions and the red minium particles deposit on the negatively charged surface regions. In recent years, charged toners for copying machines were used as decorating media (Klapper *et al*. 1987; Laurell *et al*. 1992; Wang *et al*. 1993). NLCs were first applied by Furuhata & Toriyama (1973), who revealed ferroelectric 180° domains in polar cuts of TGS. This method was further developed by a Russian group in the Shubnikov Institute of Crystallography, Moscow, and applied to polar cuts of various ferroelectrics (see, for example, Tikhomirova *et al*. 1980). The same group showed that the NLC method is also capable of revealing 180° domains in non-polar cuts (parallel to the spontaneous polarization) of KTP (Ivanov *et al*. 1993, 1994). This technique does not require heating or cooling of the crystal, but it needs freshly cleaved surfaces that are not yet polluted by the adsorption of impurities and neutralized by vagabonding charges.

The experimental procedure is rather simple: the nematic-crystal fluid is spread over the freshly cleaved surface. The substrate crystal with the NLC film is studied by polarizing microscopy (crossed polarizers) in transmission. The molecules of the NLC film adopt ordered, and therefore birefringent, orientation states which differ for substrate regions of opposite polarity. This leads to birefringent 'liquid-crystal domains' ('NLC domains') with different optical extinction orientations. The NLC domains mark the 180° domains of the underlying substrate crystal. Usually the extinction positions are different for the substrate and for the NLC domains. In most cases the optical contrast of the NLC domains and their boundaries is strongest when the substrate is in the extinction position and does not contribute to the light transmitted through the crossed polarizers. Often, an optimal contrast of the NLC domains is found for deviations of a few degrees from the substrate extinction position.

3. X-ray topographic imaging of inversion boundaries

The first X-ray topographic characterization of inversion twins and inversion boundaries was carried out by A. R. Lang, who studied the Dauphiné and Brazil twins of natural quartz (Lang 1967*a*, *b*; Lang & Miuskov 1969). Brazil twins can be considered as inversion twins, whereas the Dauphiné-twin law is represented by twofold axis along the trigonal axis [001] of quartz. For X-ray reflections of type $hh\bar{2}hl$ and $hh\bar{2}\bar{h}0$, however, Dauphiné twins show the same X-ray topographic imaging behaviour as inversion twins.

Inversion domains can only be visualized by X-ray topographic domain contrast, if Friedel's rule, $|F(hkl)| = |F(\bar{h}\bar{k}\bar{l})|$, is broken by anomalous scattering. By this effect, Brazil-twin domains of quartz have been imaged by Lang (1965) using Cr-$K\alpha$ radiation which is, to a sufficient extent, anomalously scattered by the Si atoms. Other examples of this 'anomalous scattering' topography are the studies of 180° domains in $BaTiO_3$ (Niizeki & Hasegawa 1964), in $LiNbO_3$ (Wallace 1970) and in $KTiOAsO_4$ (Huang *et al*. 1996).

In the case of valid Friedel's rule, inversion domains can be recognized by the imaging of their boundaries. Due to the exact parallelity of the lattices of both domains, these boundaries are usually strain-free and appear by dynamical fringe contrast corresponding to that of stacking faults. This contrast is due to the 'interbranch scattering' of dynamical X-ray wave fields and results from the phase jump of the structure amplitude at the inversion boundary: $F\exp(-\mathrm{i}\Phi) \Leftrightarrow F\exp(+\mathrm{i}\Phi)$. According to Lang (1967*a*, *b*), the total phase jump at the inversion interface is $2\Phi + 2\pi\boldsymbol{g}\cdot\boldsymbol{f}$, where $\boldsymbol{g}$ is the diffraction vector ($g = 1/d_{hkl}$) and $\boldsymbol{f}$ is the vector of the Bravais lattice displacement (fault vector) which may be encountered on crossing the boundary. (Note that the phase angle Φ depends on the origin of the coordinate system and that the phase change 2Φ results from an inversion centre located in the origin. For another choice of the origin, both Φ and $\boldsymbol{f}$ are changed in such a way that the total phase jump at the boundary remains unchanged.)

According to Lang (1967*a*, *b*), the inversion boundary is invisible ('extinct') if the total phase jump is an integer multiple of 2π:

$$2\Phi + 2\pi\boldsymbol{g}\cdot\boldsymbol{f} = 2\pi N \quad (N \text{ an integer}).$$

From this relation the fault $\boldsymbol{f}$ vector may be determined (at least approximately) by finding such reflections for which boundary contrast does not appear. If the phases of these reflections are known (e.g. by calculations based on the known crystal structure), the fault vector and information on the structure of the boundary can be derived. The fault vectors of Brazil and Dauphiné twin boundaries (in the latter case using reflections of type $hh\bar{2}\bar{h}l$ and $hh\bar{2}\bar{h}0$) were determined in this way by Lang (1967*a*, *b*). Of particular interest is the result that the fault vectors depend on the orientation of the twin interfaces. Another X-ray topographic determination of the fault vectors, using the above criterion, was performed for the (001) inversion boundaries of ferroelectric NH_4LiSO_4 (Hildmann 1980; Klapper 1987, p. 387).

4. Experimental

The KTP crystal studied in this work was grown by the flux method on a seed. The crystal was cleaved in slices along its perfect cleavage plane (100) (referred to the

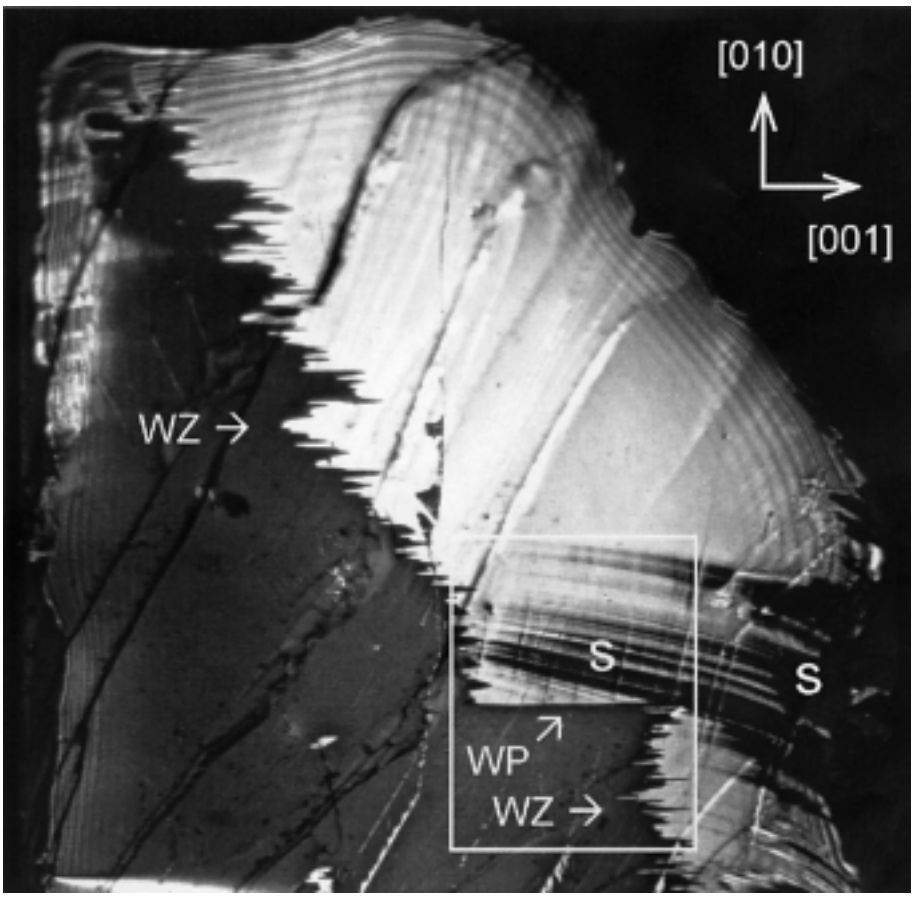

Figure 1. Freshly cleaved non-polar (100) plate of KTP (imaged section *ca.* $5.3 \times 5.3\,\mathrm{mm}^2$), with NLC film on one face, between crossed polarizers. The orientation of the KTP substrate deviates by a few degrees from its optical darkness position. WZ, zigzag (charged) 180° domain walls; WP, segment of uncharged domain wall (parallel to the polar axis [001]); S, artefacts (interruptions) of the NLC film. The fringes are optical isochromates arising from the decrease of film thickness toward the periphery of the probe. The frame shows the crystal section imaged in figure 3*a*.

space group setting $Pna2_1$). Two neighbouring plates were used for the comparative investigation, one for the NLC decoration of the (common) cleavage face, the other for transmission X-ray topography. The quality of both cleaved surfaces in the regions critical for the experiment was good enough to omit the usual procedures of etching. This preserved domains from partial destruction and provided excellent coincidence of pictures obtained by NLC decoration and X-ray topography. As NLC fluid, a four-component mixture of cyanobiphenyles with positive dielectric anisotropy was used.

The X-ray topographic studies were carried out using the Lang technique (Lang 1959*a*, *b*) using Mo-$K\alpha$ radiation of a rotating-anode generator. The linear absorption coefficient of KTP for this radiation is $\mu_0 = 3.2\,\mathrm{mm}^{-1}$. This resulted in a moderate absorption $\mu_0 t = 1.6$ for the investigated plate of thickness $t \approx 0.5\,\mathrm{mm}$.

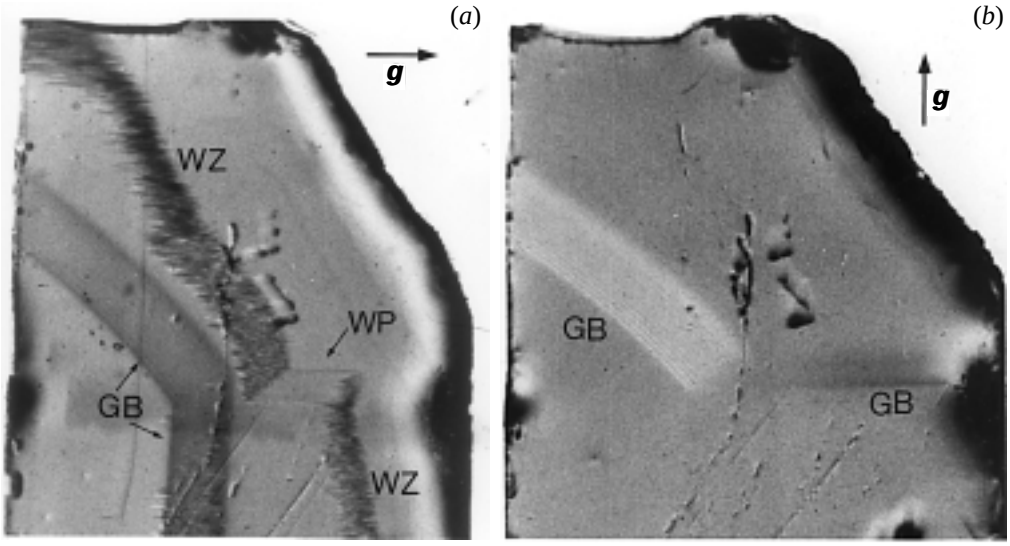

Figure 2. X-ray topographs (Mo-$K\alpha$ radiation) of the cleavage partner of the KTP plate shown in figure 1 ((100)-plate, section $5.3 \times 5.3\,\mathrm{mm}^2$, thickness *ca.* 0.5 mm): (*a*) reflection 004; (*b*) reflection 040. WZ, zigzag domain boundary; WP, segment of uncharged domain boundary; GB, growth-sector boundaries.

The topographs were recorded on the fine-grained X-ray film Structurix D4 (Agfa-Gevaert).

5. Results and discussion

Figure 1 shows an NLC decorated non-polar (100) cleavage face of KTP. Apart from some artefacts of the NLC film, two large regions of different optical brightness, belonging to two antipolar 180° domains of the KTP substrate, are recognized. One of the two NLC regions is close to the optical extinction orientation. Consequently, the boundary between these two regions appears by strong optical contrast. It is essentially an irregular zigzag-like boundary (WZ) with an average orientation between 60° and 90° to the polar axis [001], containing large line segments parallel to [001]. One of these uncharged segments (WP) is rather long and exactly parallel to the polar axis. The zigzag-like and spiky geometry is typical for charged ('electrically forbidden') boundaries, because it reduces their local charge density.

In figure 2 X-ray topographs of the other cleavage partner are presented. The plate is essentially dislocation free. Apart from some surface damage and growth-sector boundaries (GB) it contains the inversion boundary, which is clearly imaged in reflection 004 but completely invisible in reflection 040. The course of this boundary corresponds closely to that of the boundary in figure 1, but its X-ray topographic contrast appears rather wide and diffuse compared with the sharply defined boundary visible in figure 1. In contrast to the surface decoration methods, transmission X-ray topography projects the bulk of the crystal. This leads to a band-like image of the boundary, which is structured according to its zigzag course. The segment WP, however, defines an extended planar defect of *ca.* 1 mm length, inclined by roughly 40° against the specimen normal. It appears by dynamical fringe contrast (figure 3*a*)

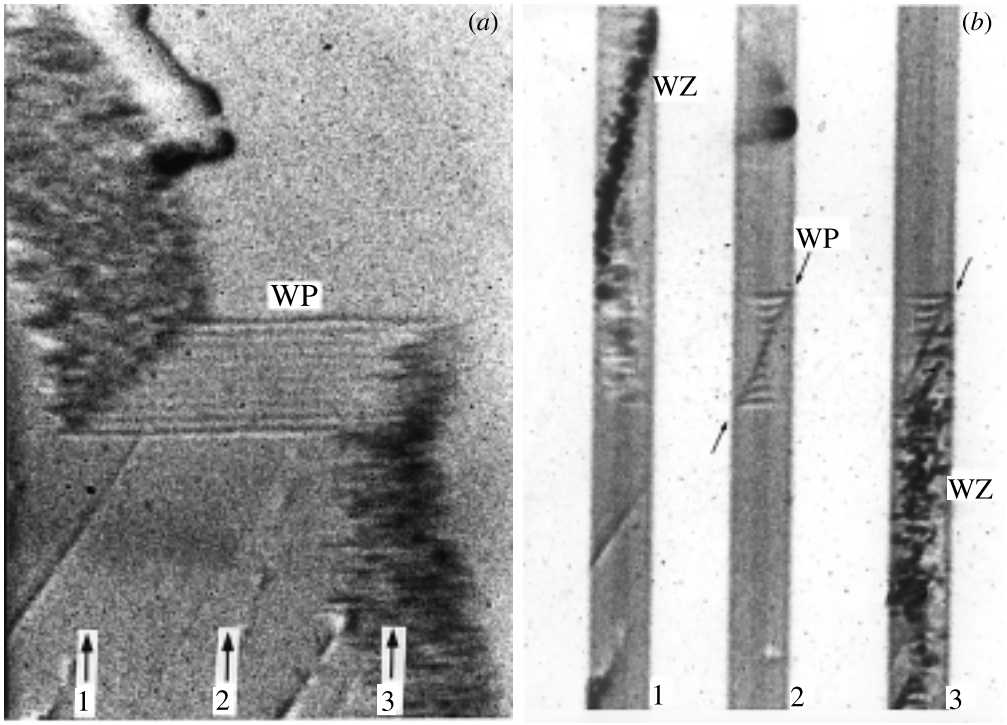

Figure 3. (*a*) Enlarged section (*ca.* 1.8×2.5 mm^2, marked in figure 1 by the frame) of topograph figure 2*a*, showing the dynamical fringe contrast of the uncharged 180° boundary segment WP. The arrows indicate the positions of the section topographs of (*b*). (*b*) Section topographs through the zigzag parts WZ and the parallel segment WP of the inversion boundary.

without any indication of lattice distortions. The undistorted 'hourglass' pattern of the planar fault in section topograph 2 of figure 3*b* confirms the absence of long-range strain and that the lattices of the domains separated by the boundary are exactly parallel to each other, as is expected for this kind of 180° walls.

The contrast of the boundary vanishes completely in reflection 040. This is expected for all reflections $hk0$ of the zone [001] (twofold polar axis). The structure amplitudes of these reflections are real and, therefore, a phase jump not equal to $2\pi N$ across the inversion boundary does not occur. In addition, for symmetry reasons a fault vector component normal to the twofold axis does not occur either, so that the total phase change across the boundary is zero or an integer multiple of 2π.

The rather strong contrast of the boundary in reflection 004 indicates the presence of a considerable phase jump. Topographs in other 'polar' reflections hkl ($l \neq 0$), however, are not available at present. They will be obtained in future with the aim of performing a fault-vector analysis similar to that carried out by Lang (1967*a*, *b*) for Brazil-twin boundaries in quartz and by Hildmann (1980) and Klapper (1987) for ferroelectric domain boundaries in NH_4LiSO_4.

This study was supported by the Deutsche Forschungsgemeinschaft by the grant of a visiting fellowship to N.R.I.

References

Furuhata, Y. & Toriyama, K. 1973 New liquid-crystal method of revealing ferroelectric domains. *Appl. Phys. Lett.* **23**, 361–362.

Hildmann, B. O. 1980 Ferroelektrische: ferroelastische Eigenschaften, Phasenumwandlungen und Kristallstrukturen von NH_4LiSO_4. Thesis, Technical University of Aachen.

Hu, Z. W., Thomas, P. A. & Risk, W. P. 1996 Periodic domain inversion in poled $KTiOPO_4$ via high-resolution X-ray topography and diffraction space mapping. *J. Phys.* D **29**, 2696–2704.

Hu, Z. W., Thomas, P. A. & Huang, P. Q. 1997 High-resolution X-ray diffraction and topographic study of ferroelectric domains and absolute structural polarity of $KTiOPO_4$ via anomalous scattering. *Phys. Rev.* **56**, 8559–8565.

Huang, X. R., Jiang, S. S., Liu, W. J., Wu, X. S., Feng, D., Wang, Z. G., Han, Y. & Wang, J. Y. 1996 Contrast of ferroelastic and ferroelectric domains in white-beam X-ray topographs. *J. Appl. Cryst.* **29**, 371–377.

Ivanov, N. R., Tikhomirova, N. A., Ginzberg, A. V., Chumakova, S. P., Osadchij, S. M. & Nikiruj, E. Ya. 1993 Static domain structure of ferroelectric flux-grown $KTiOPO_4$ crystals. *Ferroelectrics Lett.* **15**, 127–132.

Ivanov, N. R., Tikhomirova, N. A., Ginzberg, A. V., Chumakov, S. P., Eknadiosyants, E. I., Borodin, V. Z., Pinskaya, A. N., Babanskikh, V. A. & D'yakov, V. A. 1994 Domain structure of $KTiOPO_4$ crystals. *Crystallogr. Rep.* **39**, 593–599.

Klapper, H. 1987 X-ray topography of twinned crystals. In *Progr. Crystal Growth and Charact.*, vol. 14, pp. 367–401. Oxford: Pergamon.

Klapper, H., Hahn, Th. & Chung, S. J. 1987 Optical, pyroelectric and X-ray topographic studies of twin domains and twin boundaries in $KLiSO_4$. *Acta Crystallogr.* B **43**, 147–159.

Kundt, A. 1883 Ueber eine einfache Methode zur Untersuchung der Thermo-, Actino- und Piezoelektrizitaet der Krystalle. *Annln Phys.* **20**, 592–601.

Lang, A. R. 1959*a* Studies of individual dislocations in crystals by X-ray diffraction microradiography. *J. Appl. Phys.* **30**, 1748–1755.

Lang, A. R. 1959*b* The projection topograph: a new method in X-ray diffraction microradiography. *Acta Crystallogr.* **12**, 249–250.

Lang, A. R. 1965 Mapping Dauphiné and Brazil twins in quartz by X-ray topography. *Appl. Phys. Lett.* **7**, 168–170.

Lang, A. R. 1967*a* Some recent applications of X-ray topography. *Adv. X-ray Analysis* **10**, 91–107.

Lang, A. R. 1967*b* Fault surfaces in alpha quartz: their analysis by X-ray diffraction contrast and their bearing on growth history and impurity distribution. In *Crystal growth* (ed. H. S. Peiser), pp. 833–838. Oxford: Pergamon.

Lang, A. R. & Miuskov, V. F. 1969 Defects in natural and synthetic quartz. In *Growth of crystals* (ed. N. N. Sheftal), vol. 7, pp. 112–123. New York: Consultants Bureau.

Laurell, F., Roelofs, M. G., Bindloss, W., Hsiung, H., Suna, A. & Bierlein, J. D. 1992 Detection of ferroelectric domain reversal in $KTiOPO_4$ waveguides. *J. Appl. Phys.* **71**, 4664–4670.

Niizeki, N. & Hasegawa, M. 1964 Direct observation of antiparallel 180° domains in $BaTiO_3$ by anomalous dispersion method. *J. Phys. Soc. Japan* **46**, 550–554.

Satyanarayan, M. N. & Bhat, H. L. 1997 Influence of growth below and above T_c on the morphology and domain structure in flux-grown KTP crystals. *J. Crystal Growth* **181**, 281–289.

Satyanarayan, M. N., Bhat, H. L. & Sherwood, J. N. 1995 Observation of ferroelectric domains in flux-grown $KTiOPO_4$ crystals. *Ferroelectrics Lett.* **19**, 19–24.

Tikhomirova, N. A., Pikin, S. A., Shuvalov, L. A., Dontsova, L. I., Popov, E. S., Shilnikov, A. V. & Bulatova, L. G. 1980 Visualization of static and the dynamics of domain structure in triglycine sulfate by liquid crystals. *Ferroelectrics* **29**, 145–156.

Wallace, C. A. 1970 The display of twinning in lithium niobate by X-ray diffraction topography. *J. Appl. Crystallogr.* **3**, 546–547.

Wang, S., Dudley, M., Cheng, L. K., Bierlein, J. D. & Bindloss, W. 1993 Imaging of ferroelectric domains in $KTiOPO_4$ single crystals by synchrotron X-ray topography. *Ferroelectric Thin Films III Symp.* In *Mater. Res. Soc. Symp. Proc.* **310**, 29–34.